

# GYRO Performance on MPP Systems

**J. Candy**

**General Atomics, San Diego, CA**

**M.R. Fahey**

**Oak Ridge National Laboratory, Oak Ridge, TN**

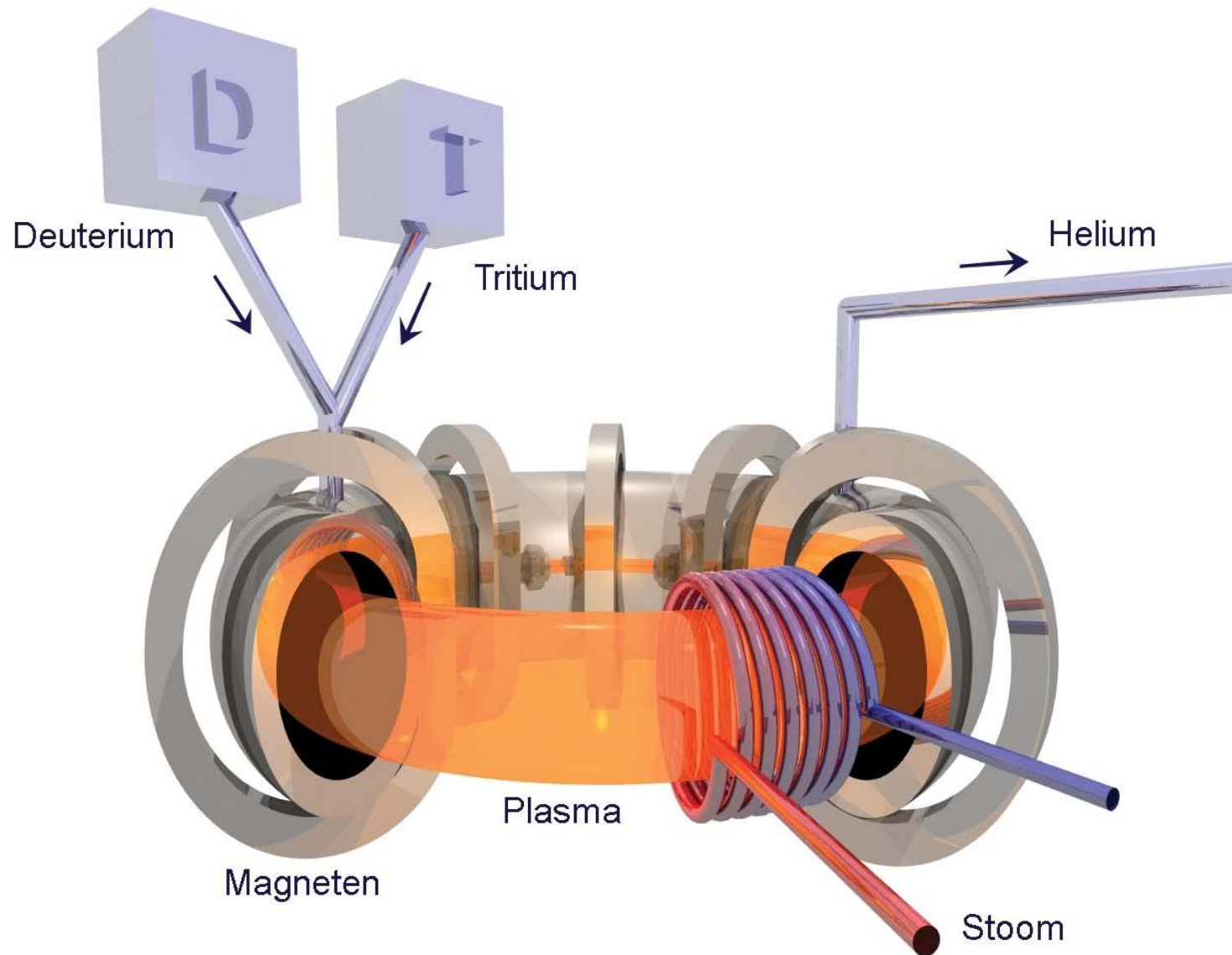
Cray User Group 2005 Meeting

*Petroglyphs to Petaflops*

Albuquerque, NM

16–19 May 2005

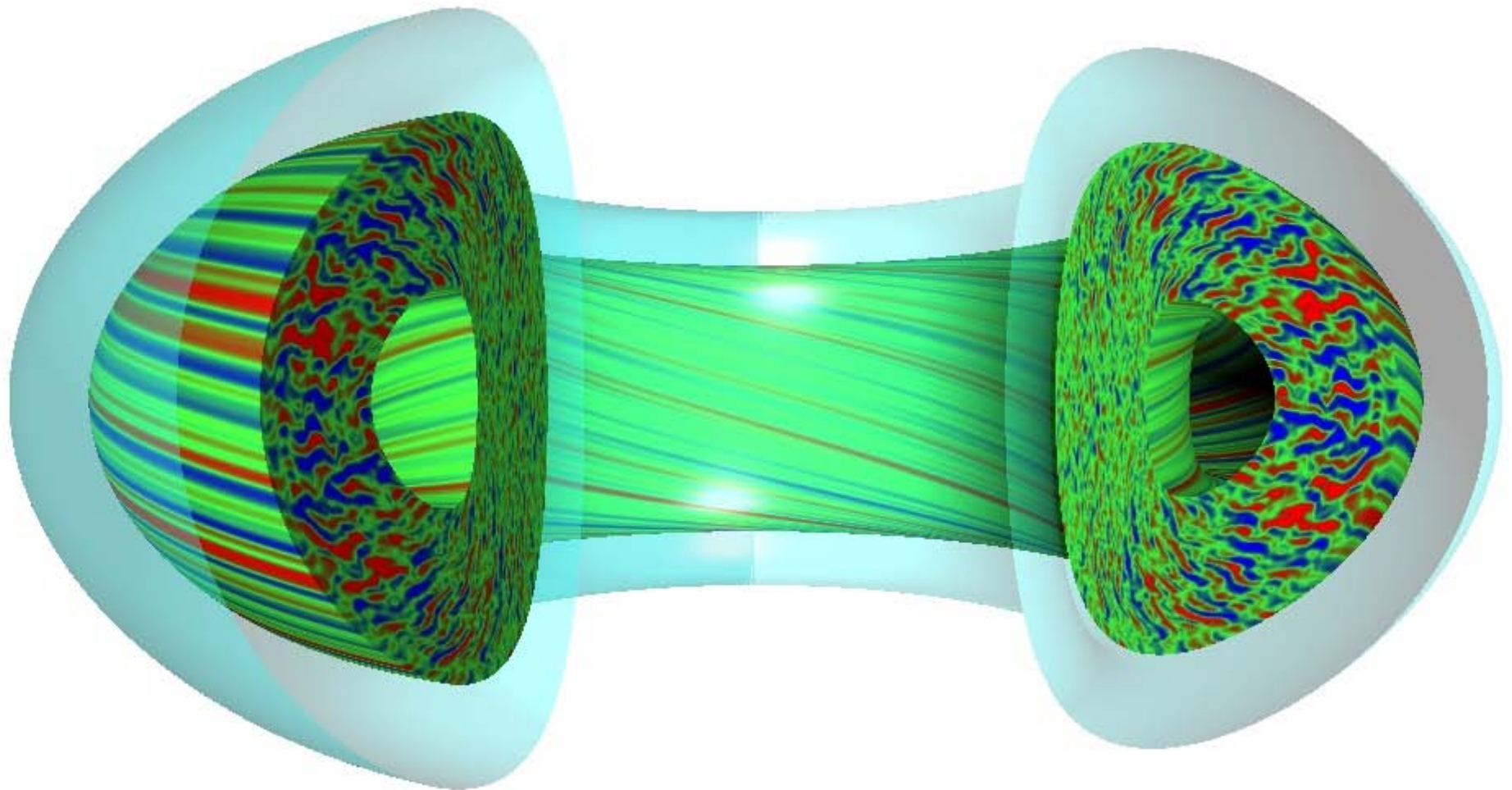
# The Most Promising Concept for Power Production by Fusion Reactions is the Tokamak



# The Construction of a Tokamak Burning Plasma Facility is a Prudent Scientific and Humanitarian Undertaking



# The Gyrokinetic-Maxwell Equations Provide the Foundation for Direct Numerical Simulation of Plasma Turbulence



# The Gyrokinetic Equations Replace the Older, Simpler Gyrofluid Model (below)

$$\frac{dn}{dt} + [\frac{1}{2} \hat{V}_\perp^2 \mathbf{v}_\Psi] \cdot \nabla T_\perp + B \nabla_\parallel \frac{u_\parallel}{B} - \left( 1 + \frac{\eta_\perp}{2} \hat{V}_\perp^2 \right) i \omega_* \Psi + (2 + \frac{1}{2} \hat{V}_\perp^2) i \omega_d \Psi + i \omega_d (p_\parallel + p_\perp) = 0,$$

$$\frac{du_\parallel}{dt} + [\frac{1}{2} \hat{V}_\perp^2 \mathbf{v}_\Psi] \cdot \nabla q_\perp + B \nabla_\parallel \frac{p_\parallel}{B} + \nabla_\parallel \Psi + \left( p_\perp + \frac{1}{2} \hat{V}_\perp^2 \Psi \right) \nabla_\parallel \ln B + i \omega_d (q_\parallel + q_\perp + 4u_\parallel) = 0,$$

$$\begin{aligned} \frac{dp_\parallel}{dt} + [\frac{1}{2} \hat{V}_\perp^2 \mathbf{v}_\Psi] \cdot \nabla T_\perp + B \nabla_\parallel \frac{q_\parallel + 3u_\parallel}{B} + 2(q_\perp + u_\parallel) \nabla_\parallel \ln B - \left( 1 + \eta_\parallel + \frac{\eta_\perp}{2} \hat{V}_\perp^2 \right) i \omega_* \Psi + \left( 4 + \frac{1}{2} \hat{V}_\perp^2 \right) i \omega_d \Psi \\ + i \omega_d (7p_\parallel + p_\perp - 4n) + 2|\omega_d| (v_1 T_\parallel + v_2 T_\perp) = -\frac{2}{3} v_{ii} (p_\parallel - p_\perp), \end{aligned}$$

$$\begin{aligned} \frac{dp_\perp}{dt} + [\frac{1}{2} \hat{V}_\perp^2 \mathbf{v}_\Psi] \cdot \nabla p_\perp + [\hat{V}_\perp^2 \mathbf{v}_\Psi] \cdot \nabla T_\perp + B^2 \nabla_\parallel \frac{q_\perp + u_\parallel}{B^2} - \left[ 1 + \frac{1}{2} \hat{V}_\perp^2 + \eta_\perp \left( 1 + \frac{1}{2} \hat{V}_\perp^2 + \hat{V}_\perp^2 \right) \right] i \omega_* \Psi \\ + \left( 3 + \frac{3}{2} \hat{V}_\perp^2 + \hat{V}_\perp^2 \right) i \omega_d \Psi + i \omega_d (5p_\perp + p_\parallel - 3n) + 2|\omega_d| (v_3 T_\parallel + v_4 T_\perp) = \frac{1}{3} v_{ii} (p_\parallel - p_\perp), \end{aligned}$$

$$\frac{dq_\parallel}{dt} + (3 + \beta_\parallel) \nabla_\parallel T_\parallel + \sqrt{2} D_\parallel |k_\parallel| q_\parallel + i \omega_d (-3q_\parallel - 3q_\perp + 6u_\parallel) + |\omega_d| (v_5 u_\parallel + v_6 q_\parallel + v_7 q_\perp) = -v_{ii} q_\parallel,$$

$$\begin{aligned} \frac{dq_\perp}{dt} + [\frac{1}{2} \hat{V}_\perp^2 \mathbf{v}_\Psi] \cdot \nabla u_\parallel + [\hat{V}_\perp^2 \mathbf{v}_\Psi] \cdot \nabla q_\perp + \nabla_\parallel \left( T_\perp + \frac{1}{2} \hat{V}_\perp^2 \Psi \right) + \sqrt{2} D_\perp |k_\parallel| q_\perp + \left( p_\perp - p_\parallel + \hat{V}_\perp^2 \Psi - \frac{1}{2} \hat{V}_\perp^2 \Psi \right) \nabla_\parallel \ln B \\ + i \omega_d (-q_\parallel - q_\perp + u_\parallel) + |\omega_d| (v_8 u_\parallel + v_9 q_\parallel + v_{10} q_\perp) = -v_{ii} q_\perp. \end{aligned}$$

# Gyrokinetic Equations Look Deceptively Simple

$$\frac{\partial f}{\partial t} = \mathcal{L}_a f + \mathcal{L}_b \langle \Phi \rangle + \{f, \langle \Phi \rangle\}$$
$$\mathcal{F}\Phi = \int \int dv_1 dv_2 \langle f \rangle$$

- $f$  is the **gyrocenter** distribution (measures the deviation from a Maxwellian), and  $\Phi(\mathbf{r}) = [\phi, A_{\parallel}]$  are EM fields.
- $\mathcal{L}_a$ ,  $\mathcal{L}_b$  and  $\mathcal{F}$  are linear operators
- $\langle \cdot \rangle$  is a **gyroaveraging operator**
- The function  $f(\mathbf{r}, v_1, v_2)$  is discretized over a 5-dimensional grid

# Eulerian Schemes Solve the GKM Equations on a Fixed Grid

$$f(r, \tau, n_{\text{tor}}, \lambda, E) \longrightarrow f(i, j, n, k, e)$$

$$i = 1, 2, \dots, N_i$$

$$j = 1, 2, \dots, N_j$$

$$n = 1, 2, \dots, N_n$$

$$k = 1, 2, \dots, N_k$$

$$e = 1, 2, \dots, N_e$$

**BASE DISTRIBUTION:**  $f([n], \{e, k\}, i, j)$  (1)

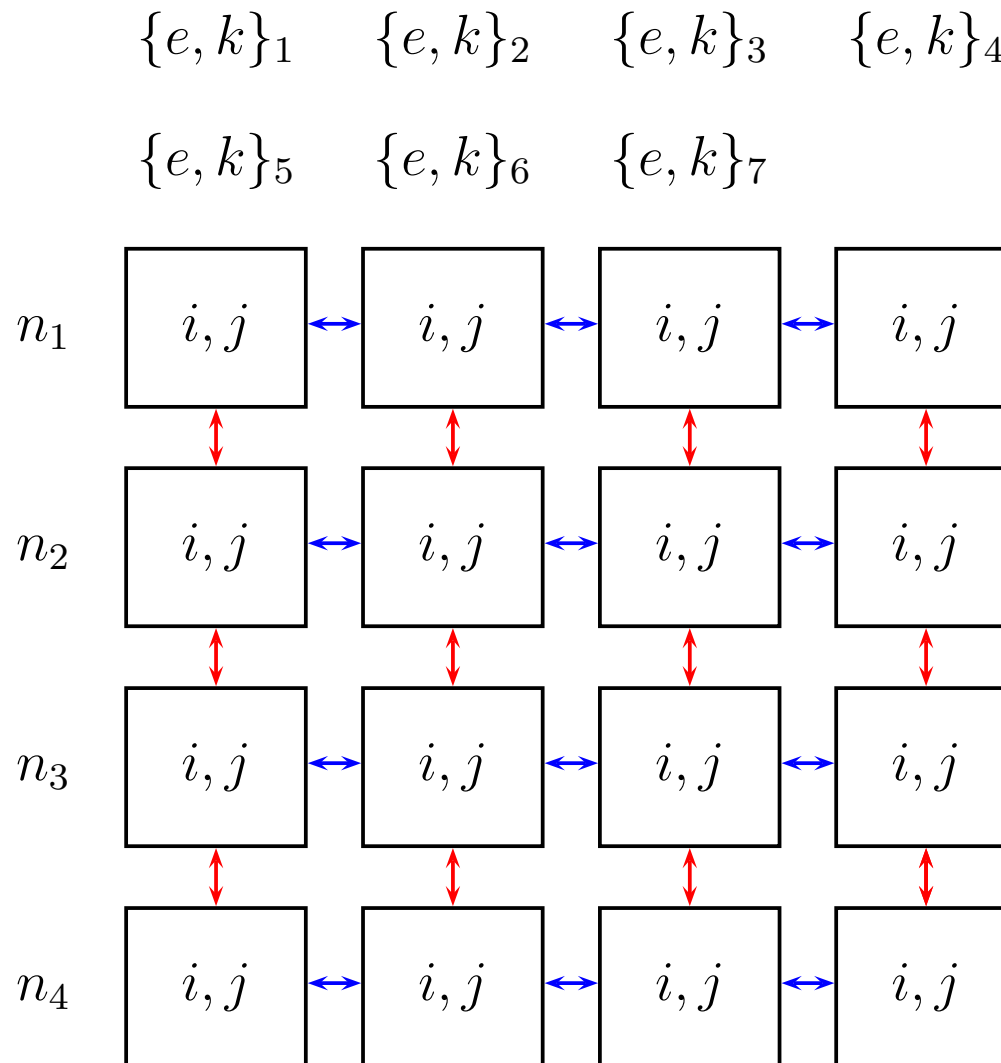
# Distribution requirements for different code stages (i.e., evaluation of different operators)

- The distribution of an index across processors is incompatible with the evaluation of operators on that index
- For example, a derivative in  $r$  requires that all  $i$  should be on a processor

Stage	On-processor indices
Linear with field solve	$i, j$
Pitch-angle scattering	$j, k$
Energy diffusion	$e$
Nonlinear	$i, n$



# Base Distribution: Velocity-Space over Columns and Toroidal Modes over Rows.



## 3-index Row Transpose: Symbolic Notation

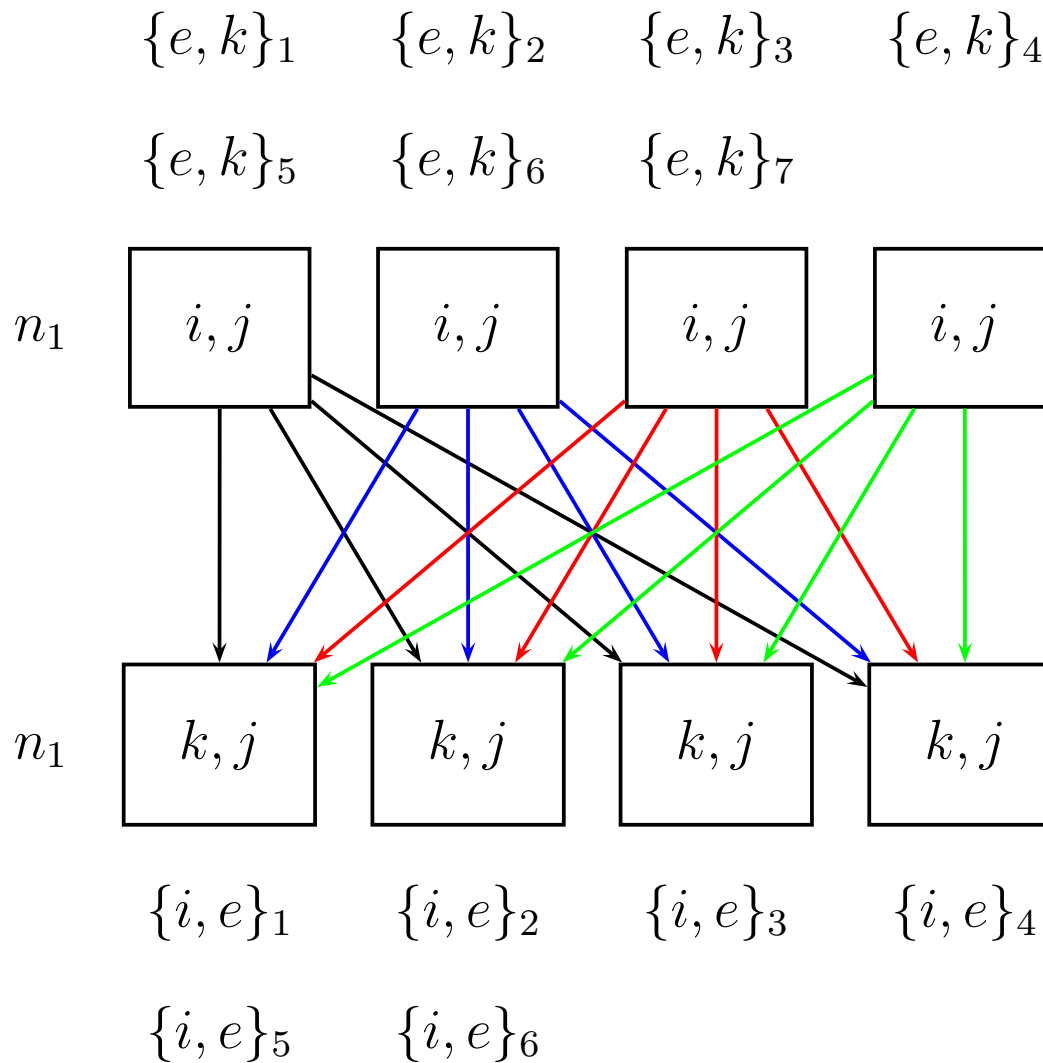
We can define a generalized 3-index transpose operator,  $R$ , which acts individually on processor rows

$$R : \{e, k\}, i \longrightarrow \{i, e\}, k$$

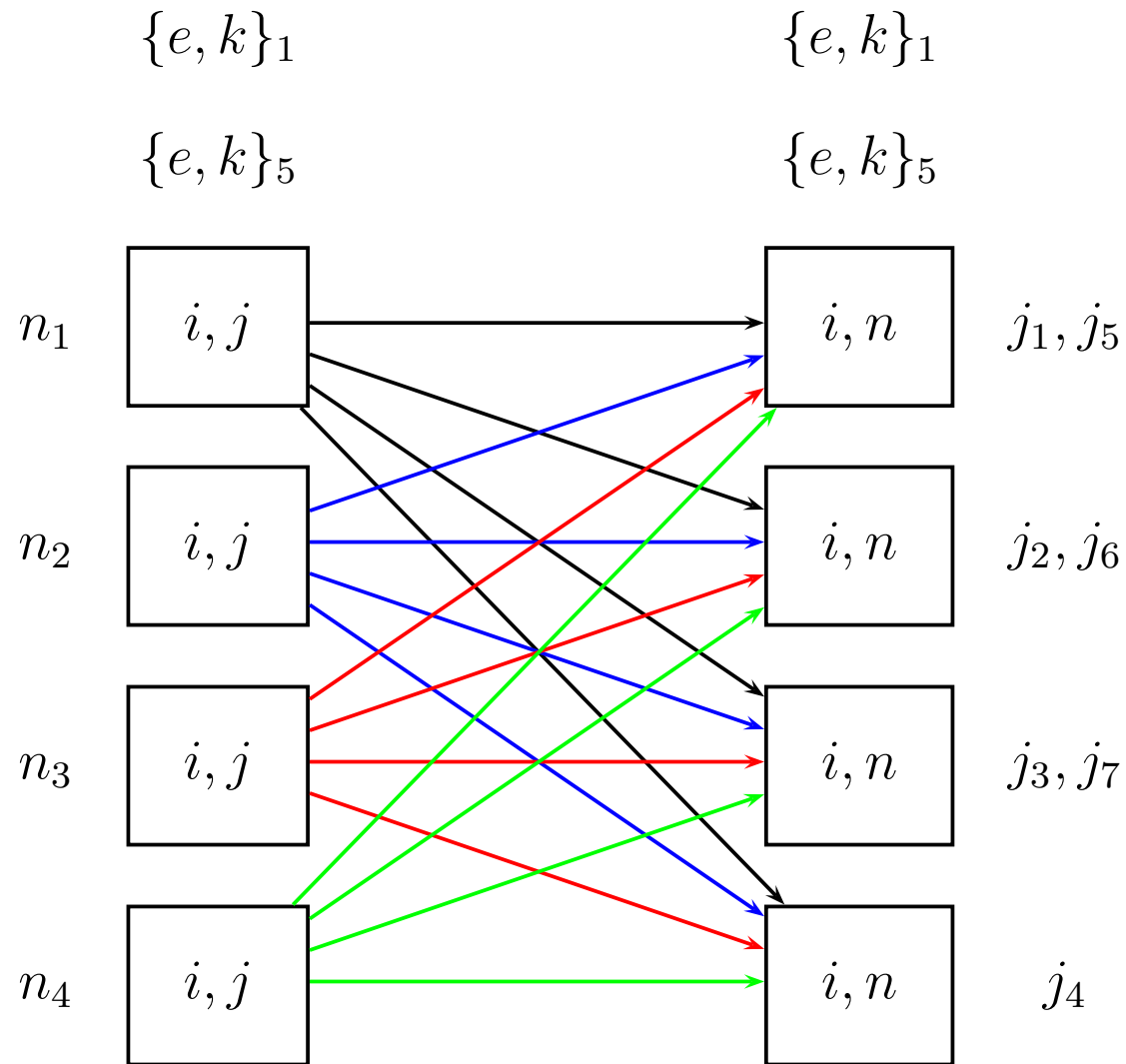
The omitted index,  $j$ , is left on-processor. Because there are three indices, three applications of the operator  $R$  yields the identity:

$$\begin{aligned} R^3 : \{e, k\}, i &= R^2 : \{i, e\}, k \\ &= R : \{k, i\}, e \\ &= \{e, k\}, i \end{aligned}$$

# 3-index Row Transpose: Schematic Description



# 2-index Column Transpose: Schematic Description



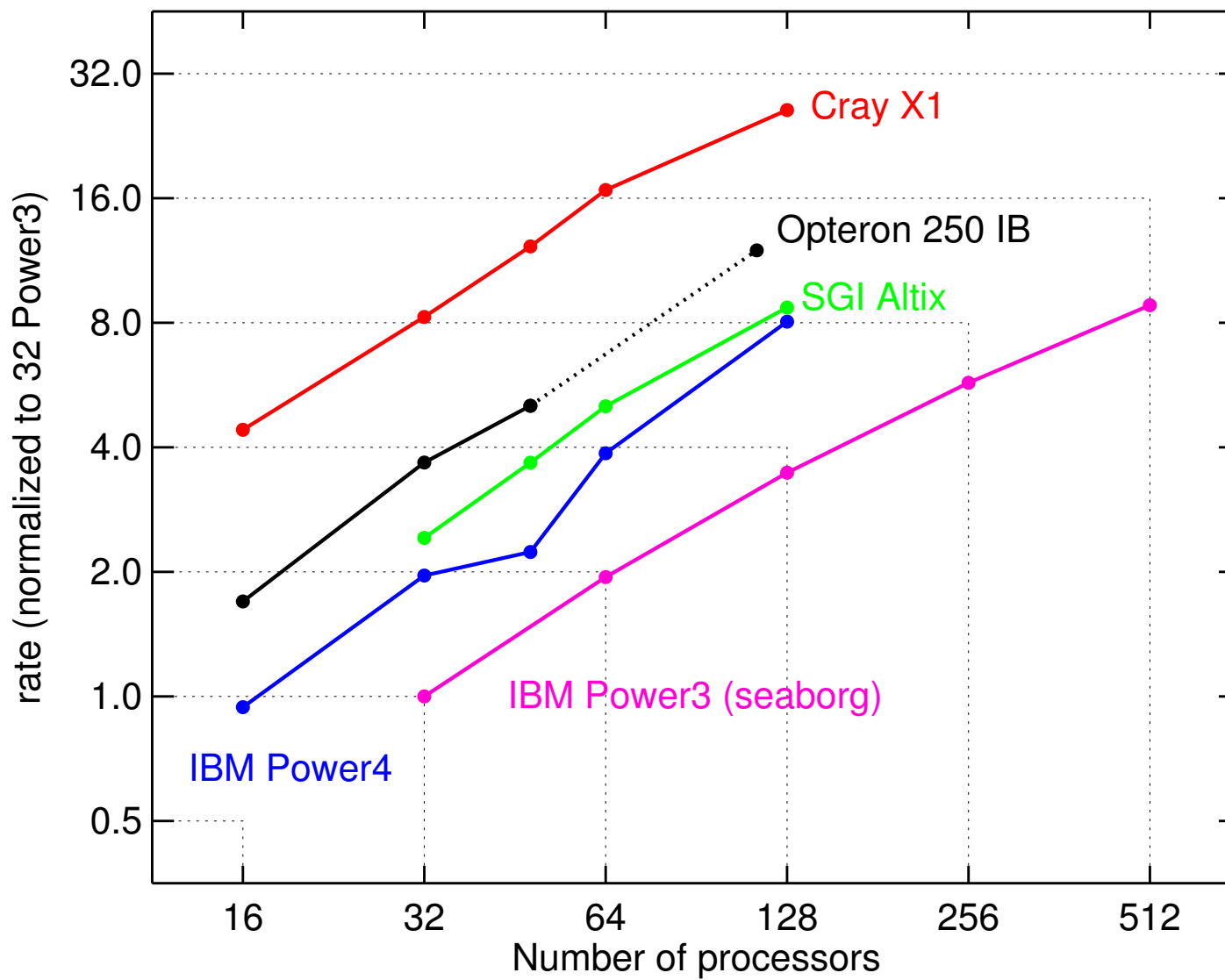
# Distributions of Indices in Each Stage

Stage	Distribution
Linear terms with field solve	$f([n], \{e, k\}, i, j)$
Pitch-angle scattering	$f([n], \{i, e\}, k, j)$
Energy diffusion	$f([n], \{k, i\}, e, j)$
Nonlinear	$f([j], \{e, k\}, i, n)$

Typical sizes:

$$N_n = 16 \quad N_e = 8 \quad N_k = 8 \quad N_i = 128 \quad N_j = 28$$

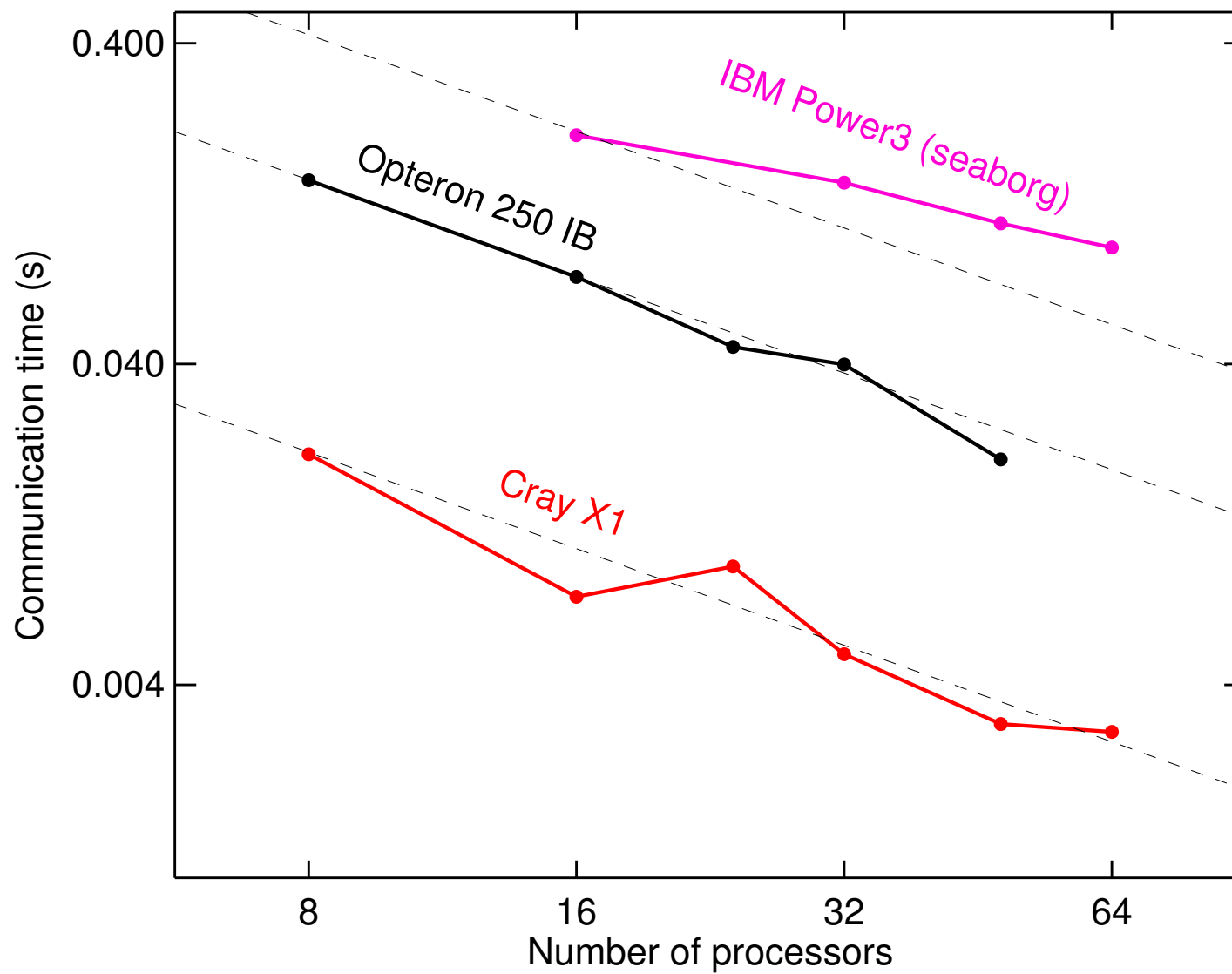
# GYRO: Overall Performance Comparison on 5 MPP Systems using the Waltz Standard Case Parameters (B1-std)



# Summary of Overall GYRO Performance

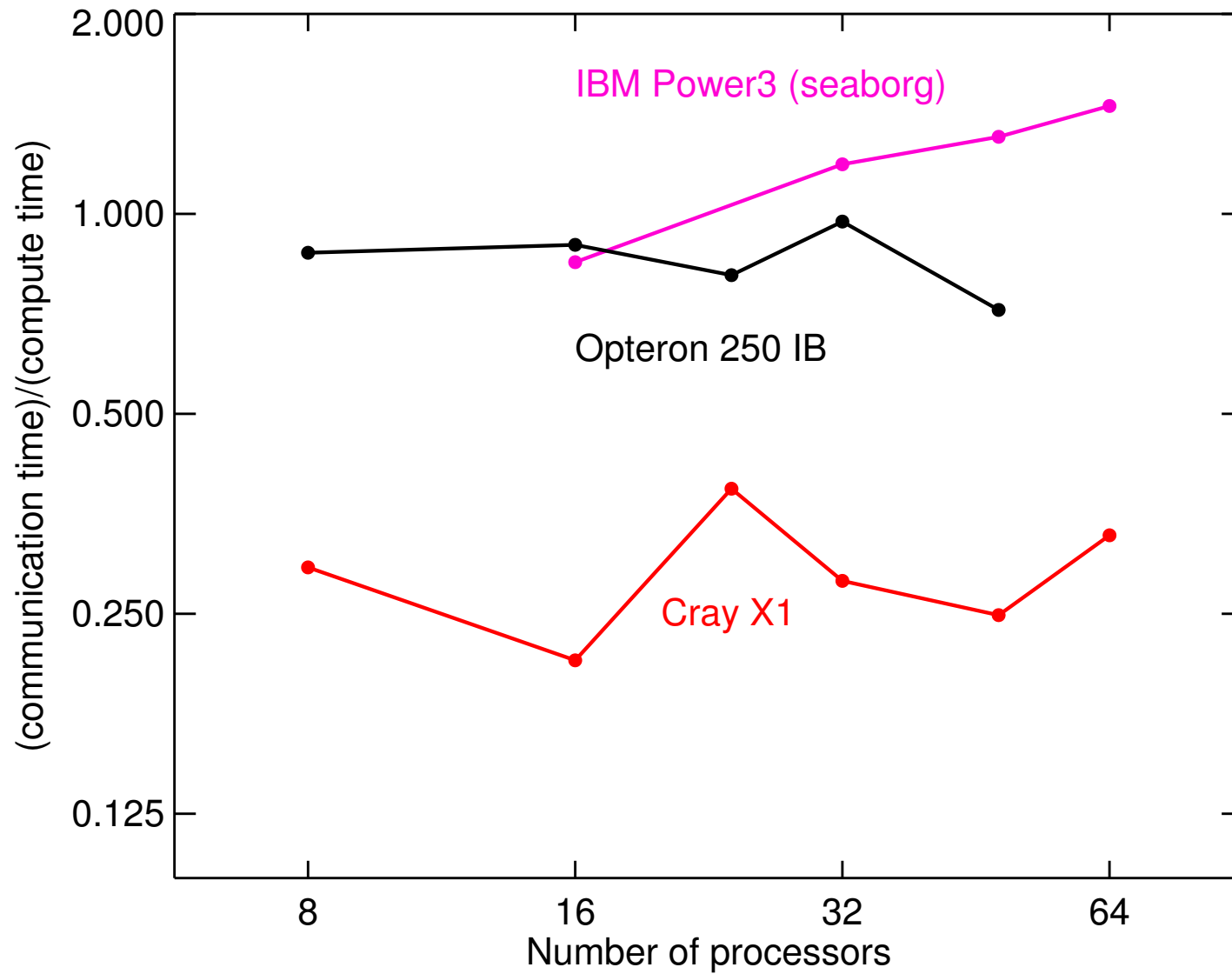
- All systems **scale well** up to and past 128 processors.
- The **Cray X1** is the hands-down winner in per-processor performance:
  - 8× the Power3
  - 4× the Power4
  - 2× the Opteron-IB
- The **IBM Power 4** is twice as fast as the IBM Power 3
- The **Opteron** cluster is four times as fast as the IBM Power 3

# Absolute Communication Time For Forward+Reverse Column Transpose (fixed problem size)





# Ratio of Communication Time to Computation Time for Evaluation of Nonlinear Terms (fixed problem size)



# Summary of Essential Results for Column Transpose Timing

- Communication **scales perfectly** on the Cray and Opteron systems
- Communication **scales reasonably well** on the IBM Power3
- The **communication-to-computation** ratio is near unity on the Opteron and Power3 systems, and about 0.25 on the Cray
- The Cray X1 is the only system for which GYRO is not significantly communication-bound.

# Preliminary Consideration for the FFT Algorithm: Libraries and Transform Length

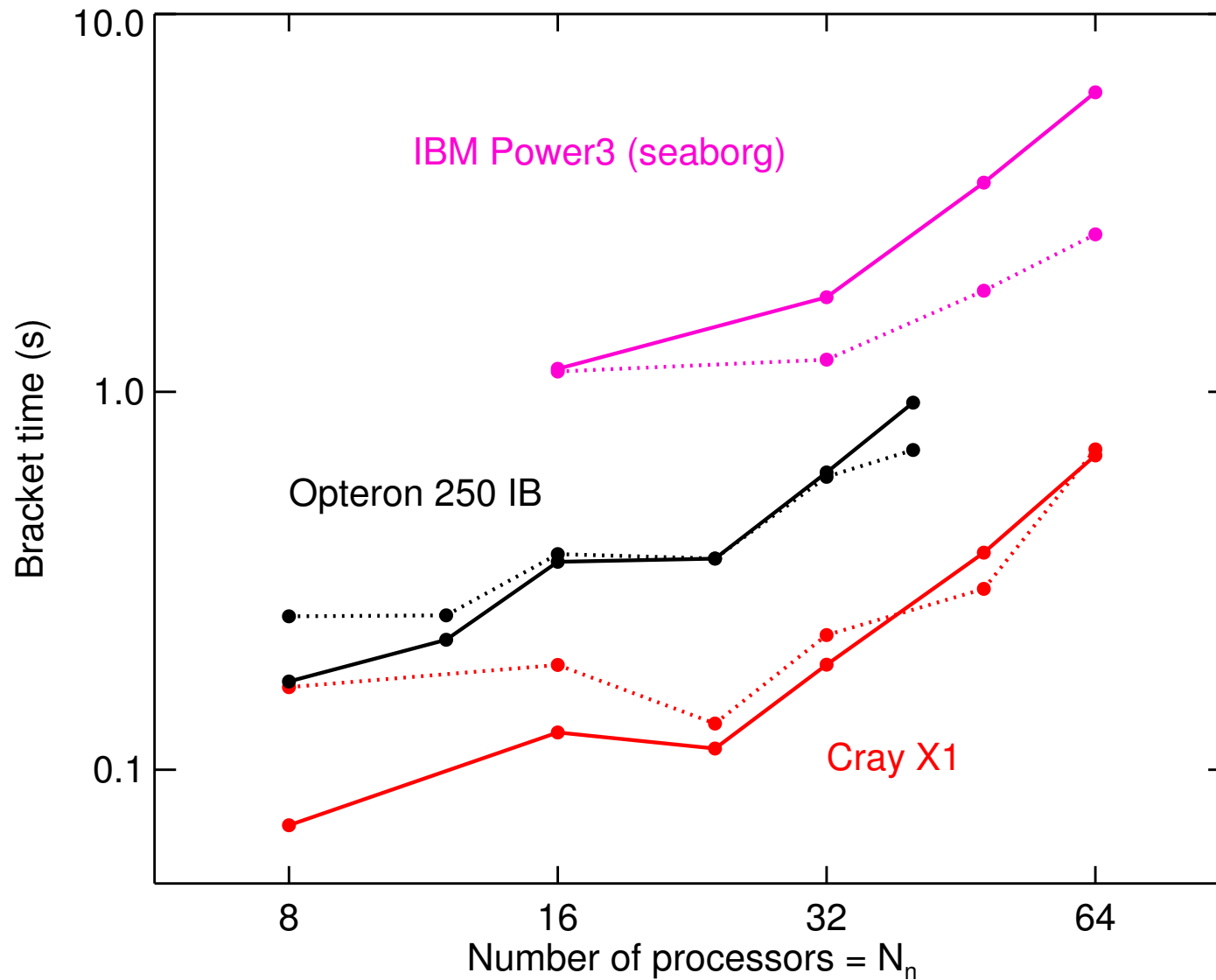
- The fields to be transformed are **complex**
- The real-space products need to be **dealiased** for **conservation** of **density**, as well as (generalized) **energy** and **enstrophy** (fluid vorticity in NS turbulence).
- We compute  $6N_i$  FFTs of length  $3N_n$  during each call
- The FFT libraries are different on each machine:
  - **FFTW 2.1.5** on the AMD
  - **ESSL** on the IBM
  - **LibSci** on the Cray

# Preliminary Consideration for the FFT Algorithm: Algebraic Structure

- The discretization uses the **Arakawa symmetrization** to enforce conservation laws

$$\begin{aligned}\{F, G\} &= \frac{\partial F}{\partial \alpha} \frac{\partial G}{\partial r} - \frac{\partial G}{\partial \alpha} \frac{\partial F}{\partial r} \\ &= \frac{1}{3} \frac{\partial}{\partial \alpha} \left( F \frac{\partial G}{\partial r} - G \frac{\partial F}{\partial r} \right) \\ &\quad + \frac{1}{3} \frac{\partial}{\partial r} \left( G \frac{\partial F}{\partial \alpha} - F \frac{\partial G}{\partial \alpha} \right) \\ &\quad + \frac{1}{3} \left( \frac{\partial F}{\partial \alpha} \frac{\partial G}{\partial r} - \frac{\partial G}{\partial \alpha} \frac{\partial F}{\partial r} \right) .\end{aligned}$$

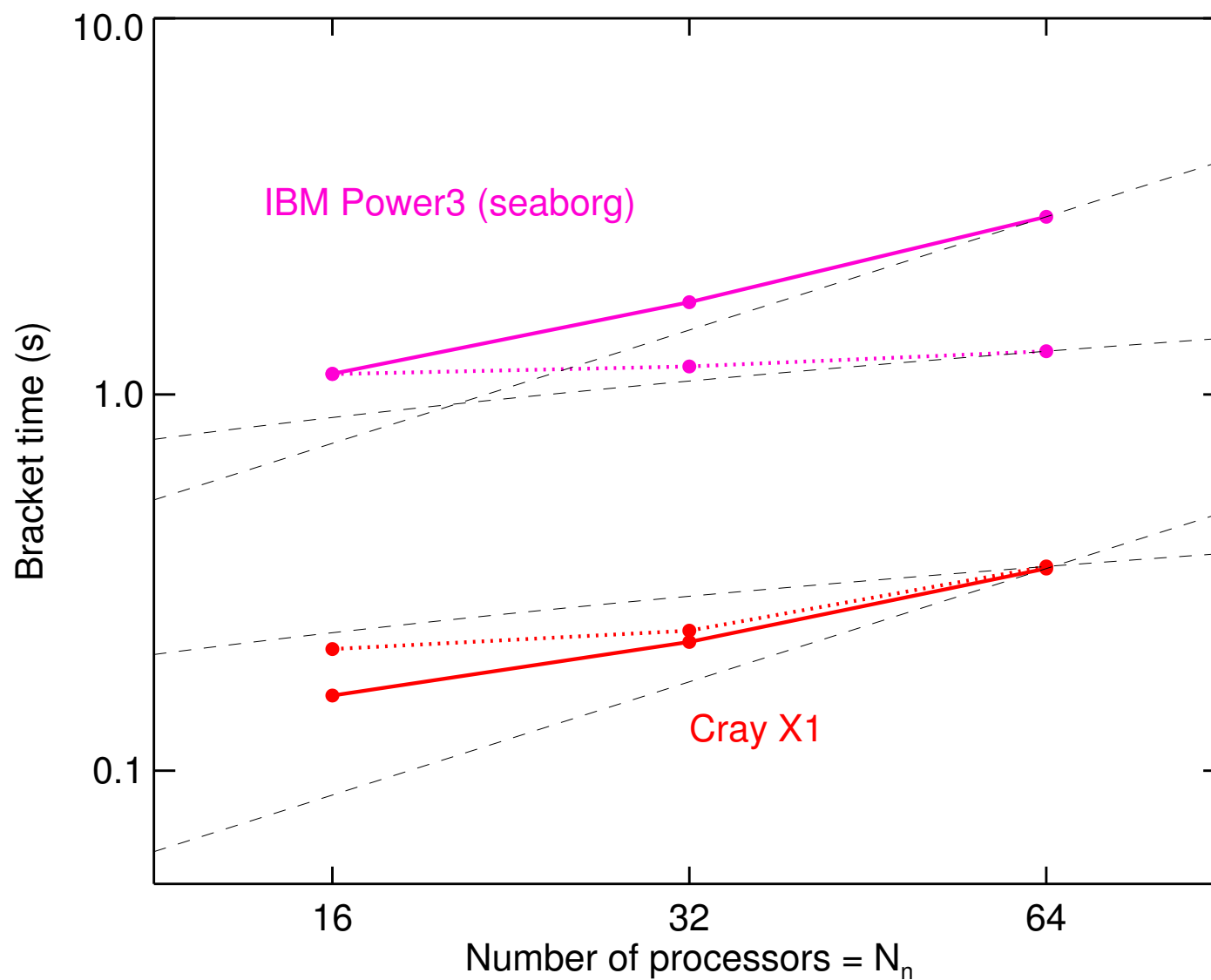
# Comparison of Direct vs. FFT Method for Poisson Bracket Evaluation: Dotted Line is FFT



# Conclusions Regarding Use of FFT Method (in place of direct method) for GYRO Simulations

- The FFT method (dotted curve) is preferred over the direct method (solid curve) for:
  - $N_n \geq 16$  modes on the IBM Power3
  - $N_n \geq 32$  modes on the AMD Opteron cluster
  - $N_n \geq 48$  modes on the Cray X1

# Comparison of Direct vs. FFT Method Using Large Poloidal Grid: Dotted Line is FFT



# Conclusions Regarding Use of FFT Method for (perfectly load balanced) GYRO Simulations

The FFT behaviours on the IBM and Cray differ.

- The **IBM FFT cost** is, surprisingly, linear in  $N_n$  over the range  $16 \leq N_n \leq 64$ .
- The **Cray FFT cost** is **comparable** to the direct cost over the range  $N_n \leq 16 \leq 64$
- We are never in a truly asymptotic  $\mathcal{O}(N_n \log N_n)$  regime for which the FFT is “spectacular”